

Tuning of the hole spin relaxation time in single self-assembled $\text{In}_{1-x}\text{Ga}_x\text{As}/\text{GaAs}$ quantum dots by electric field

Hai Wei,^{1,2} Guang-Can Guo,^{1,2} and Lixin He^{1,2, a)}

¹⁾Key Laboratory of Quantum Information, University of Science and Technology of China, Hefei, Anhui, 230026, China

²⁾Synergetic Innovation Center of Quantum Information and Quantum Physics, University of Science and Technology of China, Hefei, 230026, China

(Dated: 23 July 2014)

We investigate the electric field tuning of the phonon-assisted hole spin relaxation in single self-assembled $\text{In}_{1-x}\text{Ga}_x\text{As}/\text{GaAs}$ quantum dots, using an atomistic empirical pseudopotential method. We find that the electric field along the growth direction can tune the hole spin relaxation time for more than one order of magnitude. The electric field can prolong or shorten the hole spin lifetime and the tuning shows an asymmetry in terms of the field direction. The asymmetry is more pronounced for the taller the dot. The results show that the electric field is an effective way to tune the hole spin-relaxation in self-assembled QDs.

PACS numbers: 72.25.Rb, 73.21.La, 71.70.Ej

Because of the three-dimensional confinement, the electron and hole in self-assembled quantum dots (QDs) are only weakly coupled to the environment, and therefore have much longer spin lifetimes than their counterparts in bulk materials.^{1,2} They have thus been proposed as the quantum bits (qubits) for quantum information processes.^{3,4} Recently, the initialization, manipulation and readout of electron/hole spins in QDs have been demonstrated experimentally.⁵⁻⁸

The hole spins are expected to have long coherence time, because the hyperfine interaction between hole spin with the nuclear spins is relatively small.⁹ The main mechanism that leads to the hole spin relaxation is the spin-phonon interaction due to spin-orbit coupling (SOC).^{7,8,10-14} As we know, the Dresselhaus SOC originates from bulk inversion asymmetry (BIA)¹⁵ and Rashba SOC originates from structure inversion asymmetry (SIA).¹⁶ Therefore, it is possible to tune the SOC by applying external fields, which may change both BIA and SIA in the QDs. Recent experimental^{17,18} and theoretical^{19,20} studies have shown that the SOC strength can be enhanced by the in-plane electric and magnetic field indeed. As a consequence, the hole spin relaxation can also be tuned by the external electric field.

In this paper, we investigate the tuning of hole spin relaxation time (T_1^h) by applying an external electric field along the QDs growth direction using an atomistic empirical pseudopotential method (EPM).²¹ We find that the T_1^h can be tuned by more than one order of magnitude by the external field. It is therefore an effective way to tune the spin relaxation in self-assembled QDs.

We study the hole spin relaxation at low magnetic field ($B_z = 1$ mT), where the spin relaxation is dominant by the two-phonon process.^{11,12,22} As schematically shown in Fig. 1(a), a hole at the initial (labeled as i) state, with

energy ϵ_i , absorbs a phonon of momentum \mathbf{q} and jumps to an intermediate (s) state with energy ϵ_s . It then emits a phonon with momentum \mathbf{k} and relaxes to the final (f) state with energy ϵ_f , which has an opposite spin of the initial state. The hole spin-flip rate (τ_ν^{-1}) from the initial to the final state is given by the second-order Fermi's Golden Rule,¹²

$$\frac{1}{\tau_\nu} = \frac{2\pi}{\hbar} \sum_{\mathbf{q}, \mathbf{k}} \left[\sum_s' \left(\frac{M_{\mathbf{q}}^{is} M_{\mathbf{k}}^{sf}}{\epsilon_i - \epsilon_s + \hbar\omega_{\mathbf{q}}} + \frac{M_{\mathbf{k}}^{is} M_{\mathbf{q}}^{sf}}{\epsilon_i - \epsilon_s - \hbar\omega_{\mathbf{k}}} \right) \right]^2 \times N_q(N_k + 1) \delta(\epsilon_f - \epsilon_i - \hbar\omega_{\mathbf{q}} + \hbar\omega_{\mathbf{k}}), \quad (1)$$

where $N_q = 1/[\exp(\hbar\omega_{\mathbf{q}}/k_B T) - 1]$ is the number of phonons at the given temperature T . Only long-wave acoustic phonons are involved in the process, where $\omega_{\mathbf{q}} = c_\nu |\mathbf{q}|$, and c_ν is the sound speed for the $\nu = \text{LA}$ (longitudinal acoustic phonon) and TA (transverse acoustic phonon) modes. The $'$ in the equation indicates that the summation includes all the (intermediate) states except for the initial and final states. The hole-phonon interaction matrix elements $M_{\mathbf{q}}^{is}$ are given by:

$$M_{\mathbf{q}}^{is} = \alpha_\nu(\mathbf{q}) \langle \psi_i | e^{i\mathbf{q} \cdot \mathbf{r}} | \psi_s \rangle, \quad (2)$$

where $|\psi_i\rangle$ and $|\psi_s\rangle$ are the initial and intermediate state wave functions, respectively. $\alpha_\nu(\mathbf{q})$ is the hole-phonon coupling strength. We have considered three hole-phonon interaction mechanisms in the QDs:^{10,12} hole-acoustic-phonon interaction due to (i) the deformation potential ($\nu = \text{LADP}$), (ii) the piezoelectric field for the longitudinal mode ($\nu = \text{LAPZ}$), and (iii) the piezoelectric field for the transverse mode ($\nu = \text{TAPZ}$). $\alpha_\nu(\mathbf{q})$ and other parameters used in the calculations can be found in Ref. 12. The overall spin relaxation time $1/T_1^h = \sum_\nu 1/\tau_\nu$.

To calculate T_1^h , we use the atomistic EPM to obtain high-quality hole energy levels and wave functions.¹² We simulate a lens-shaped $\text{In}_{1-x}\text{Ga}_x\text{As}/\text{GaAs}$ QDs embedded in a cubic GaAs matrix, containing $60 \times 60 \times 60$ GaAs 8-atom unit cells, as illustrated in the Fig. 1(b). The dot

^{a)}Electronic mail: helx@ustc.edu.cn

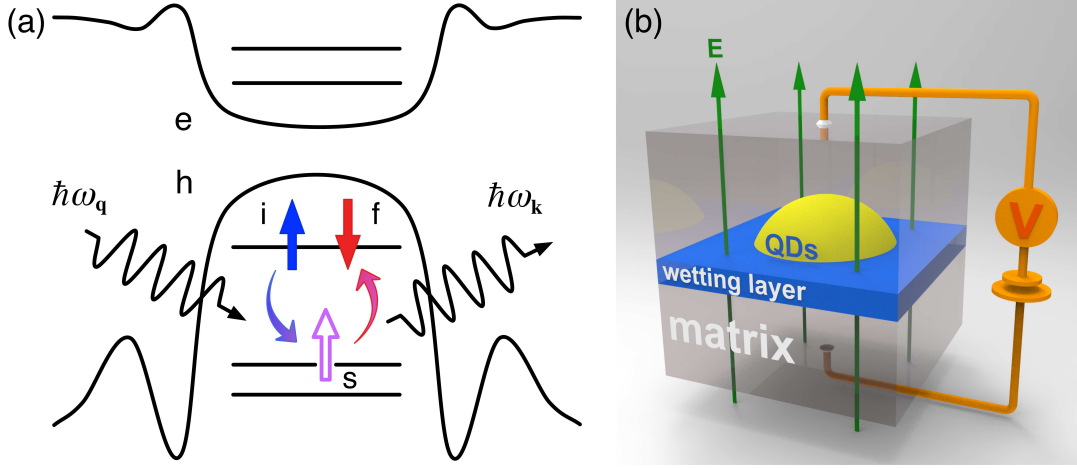


FIG. 1. (Color online) (a) The schematic show of the second-order phonon-assisted hole spin relaxation in self-assembled QDs. The i , f and s are the initial, final and intermediate levels, respectively. (b) The schematic drawing of single lens-shaped $\text{In}_{1-x}\text{Ga}_x\text{As}/\text{GaAs}$ QDs embedded in the GaAs matrix. The dot is grown on a monolayer wetting layer. The external electric field is applied along the $[001]$ ($E > 0$) or $[00\bar{1}]$ ($E < 0$) direction.

is grown along the $[001]$ direction, on the top of a monolayer wetting layer. We first obtain optimized atomic positions $\{\mathbf{R}_{n,\alpha}\}$ (α -th atom at the site n) by minimizing the total strain energy of the system (matrix+QDs) via valence force field (VFF) method.²³ The hole energy levels and wave functions are obtained by solving the following Schrödinger equation,

$$\left[-\frac{1}{2}\nabla^2 + V_{\text{epm}}(\mathbf{r}) + V_{\text{ef}}(\mathbf{r}) + \frac{1}{2}g\mu_B B_z \sigma_z \right] \psi_i(\mathbf{r}) = \epsilon_i \psi_i(\mathbf{r}), \quad (3)$$

where $V_{\text{epm}}(\mathbf{r}) = \sum_{n,\alpha} \hat{v}_\alpha(\mathbf{r} - \mathbf{R}_{n,\alpha}) + V_{\text{SO}}$ is the total screened electron-ion potential, including the superposition of all atomistic pseudopotentials $\hat{v}_\alpha(\mathbf{r})$ and the non-local spin-orbit potential V_{SO} .¹² This method naturally includes the Rashba and Dresselhaus SOC in a “first-principles” manner. V_{ef} is the external potential due to the applied electric field, along the growth direction [see Fig. 1(b)]. $E > 0$ ($E < 0$) corresponds to that the electric field points to the $[001]$ ($[00\bar{1}]$) direction. We also applied an extremely small magnetic field ($B_z = 1$ mT) along the growth direction to split the spin-up and spin-down states, where σ_z is the Pauli matrix and $g=2$ is the Lande g factor. The spin-up and spin-down energy difference caused by the magnetic field is negligible (~ 0.12 μeV).

The Schrödinger equation is solved by the linear combination of bulk bands (LCBB) method.²⁴ We use eight bands (including spin) for the hole in the calculation, which takes both the inter-valence-band coupling and the valence-conduction band coupling into account. A $6 \times 6 \times 16$ k-mesh converges the energy and wave functions very well.^{12,21} Due to the SOC, the wave functions are spin mixed, i.e. $|\psi_i\rangle = \alpha|\uparrow\rangle + \beta|\downarrow\rangle$. We regard $|\psi_i\rangle$ as a spin up (down) state if $\alpha > \beta$ ($\alpha < \beta$). To calculate T_1^h , we sum over 40 intermediate states (including spin),

which converges the results within 0.1 ms.¹²

Figure 2(a) depicts the hole relaxation time T_1^h (black solid line) at 4.2 K as a function of electric field (E) for a pure InAs/GaAs QDs with base diameter $b=20$ nm and height $h=1.5$ nm. We apply the electric field between -300 and 300 kV/cm, where the hole can still be trapped in the QDs. When no electric field is applied ($E = 0$), we find the hole spin relaxation time $T_1^h = 17.2$ ms. For $E > 0$, T_1^h decreases rapidly with the increasing E . At $E = 300$ kV/cm, T_1^h decreases to 3.5 ms. For $E < 0$, with the increasing of $|E|$, T_1^h decreases to 2.7 ms at $E = -300$ kV/cm. The short spin decay time may be useful in some cases, for example, fast spin initialization. The longest T_1^h is approximately 17.4 ms at $E = 17.2$ kV/cm.

As discussed in our previous work,¹² T_1^h is determined by two factors: one is the energy difference Δ_{sk} between the lowest level (s) and the intermediate levels (k). In this case, smaller Δ_{sk} can fasten the relaxation process. The other is minor spin component β , which reflects the spin-up and spin-down mixture due to SOC. And in this case, larger β leads to a smaller T_1^h . We find that the electric field can tune the energy spacing between the s and p_1 and p_2 level by approximately 2~4 meV, as shown in Fig. 2(b). Figure 2(c) shows the β^2 of the s (black line), p_1 (red line) and p_2 (blue line) states as functions of E . We find that the electric field can significantly change the spin mixture of the wave functions, due to the change of SOC by electric field. To determine the main mechanism that causes the change of T_1^h , we artificially fix the hole energy levels at different applied electric fields to the ones at $E=0$ kV/cm and recalculate T_1^h . The results are shown in Fig. 2(a) in the dashed red line, which are rather close to the results using the electric field dependent energy levels. This clearly suggests that spin mixture tuned by electric field plays a major rule in tuning T_1^h .

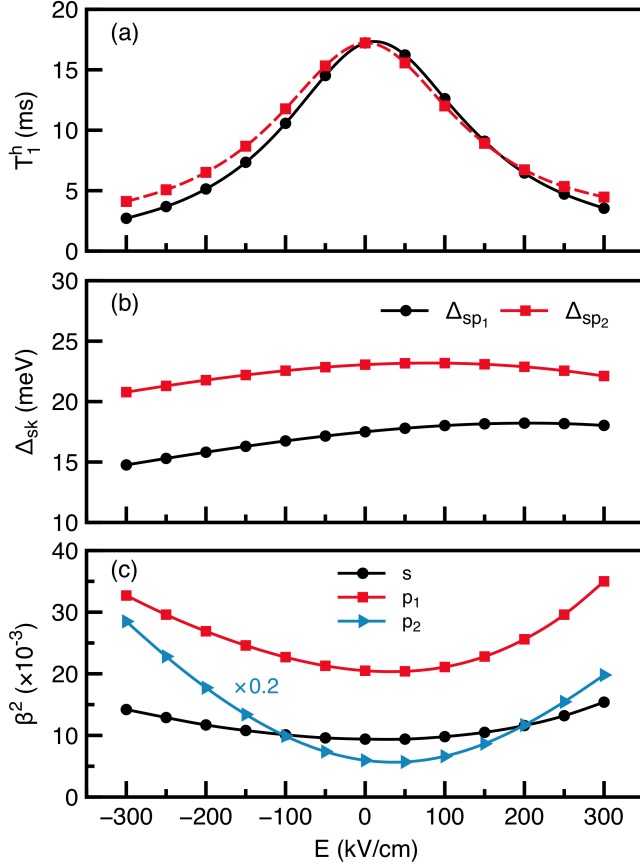


FIG. 2. (Color online) (a) Black solid line: the hole relaxation time T_1^h as a function of E in a pure InAs/GaAs QD, with $b=20$ nm, and $h=1.5$ nm. Red dashed line: same as above, but the hole energy levels are artificially fixed to those of $E = 0$ kV/cm. (b) The energy spacing between the s level and p levels as functions of E . (c) The spin mixture parameters β^2 as functions of E for the s (black), p_1 (red) and p_2 (blue) levels.

We further calculate T_1^h at 4.2 K for QDs of different geometries. Figure 3 depicts T_1^h as a function of E in pure lens-shaped InAs/GaAs QDs with fixed base diameter $b=20$ nm whereas the dot height h varies from 1.5 nm to 3.0 nm. For all QDs, the hole spin relaxation times are tuned by electric field in a very similar way. The spin relaxation time tends to decrease with $|E|$. However, for the flat QDs, the tuning of T_1^h by electric field is rather symmetric, whereas for taller dots the tuning becomes more asymmetric, because the geometry of dots themselves become more asymmetric. In all cases, the hole spin relaxation time can be tuned by more than one order of magnitude. For example, $T_1^h(-300)/T_1^h(0) = 0.11$ in the $20 \text{ nm} \times 3.0 \text{ nm}$ QDs.

We find similar results for alloy $\text{In}_{0.8}\text{Ga}_{0.2}\text{As}/\text{GaAs}$ QDs. We calculate T_1^h for the dots with base diameter $b=20$ nm, and the dot height h varying from 2.5 nm to 4.5 nm. The results are shown in Fig. 4. Remarkably, the hole spin relaxation time can be significantly

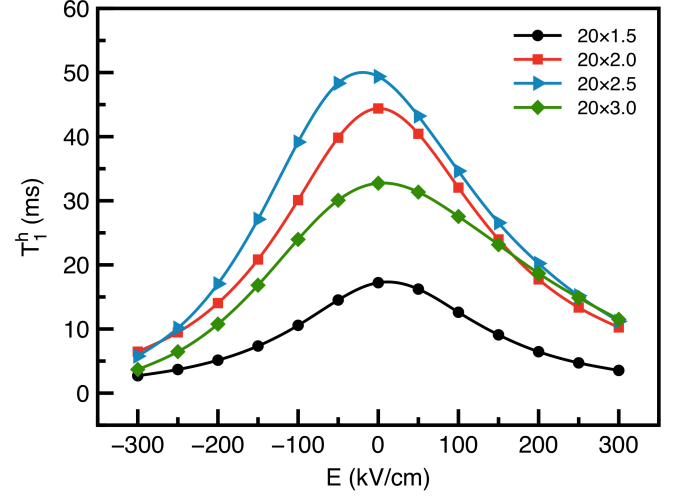


FIG. 3. (Color online) The hole spin relaxation times as functions of electric field in InAs/GaAs QDs, with dot diameter $b=20$ nm, and height $h=1.5, 2.0, 2.5$ and 3.0 nm.

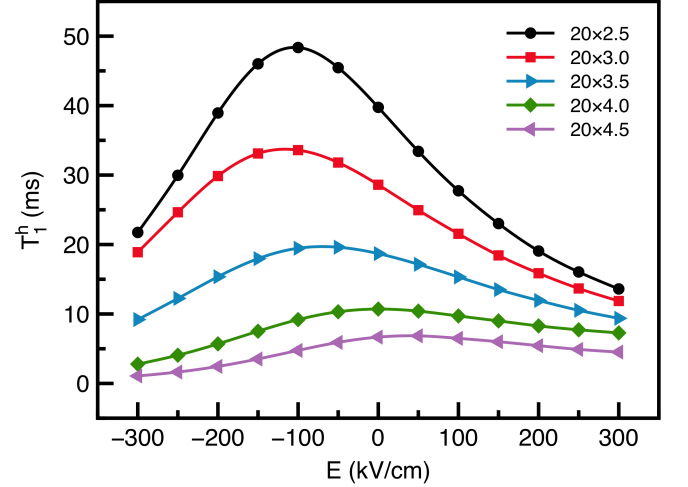


FIG. 4. (Color online) The hole spin relaxation times as functions of electric field in $\text{In}_{0.8}\text{Ga}_{0.2}\text{As}/\text{GaAs}$ QDs, with dot diameter $b=20$ nm, and height $h=2.5, 3.0, 3.5, 4.0$ and 4.5 nm.

prolonged by the electric field in the alloy dots. Take the $20 \text{ nm} \times 2.5 \text{ nm}$ QDs (black line in Fig. 4) as an example, T_1^h first increases with the negative electric field and reaches to a maximum value 48 ms at about $E_M = -100$ kV/cm. It starts to decrease when the electric field further increases. When a positive electric field is applied, T_1^h decreases monotonically. The other dots show similar behaviors. However, with the increasing of the dot height, the E_M which has the longest T_1^h generally shifts to the more positive direction, as shown in Fig. 4.

To conclude, we have investigated the tuning of hole spin relaxation in single self-assembled $\text{In}_{1-x}\text{Ga}_x\text{As}/\text{GaAs}$ QDs by electric field using an

atomistic empirical pseudopotential method. We find that the electric field can significantly increase or decrease the hole spin relaxation time in QDs, which provides an effective way to tune the hole spin relaxation time that may be useful for future device applications.

LH acknowledges support from the Chinese National Fundamental Research Program 2011CB921200 and National Natural Science Funds for Distinguished Young Scholars.

- ¹F. Meier and B. P. Zakharchenya, eds., *Optical Orientation*, Modern Problems in Condensed Matter Sciences, Vol. 8 (North-Holland, Amsterdam, 1984).
- ²L. M. Woods, T. L. Reinecke, and Y. Lyanda-Geller, *Phys. Rev. B* **66**, 161318 (2002).
- ³D. Loss and D. P. DiVincenzo, *Phys. Rev. A* **57**, 120 (1998).
- ⁴B. E. Kane, *Nature* **393**, 133 (1998).
- ⁵M. Kroutvar, Y. Ducommun, D. Heiss, M. Bichler, D. Schuh, G. Abstreiter, and J. J. Finley, *Nature (London)* **432**, 81 (2004).
- ⁶P.-F. Braun, X. Marie, L. Lombez, B. Urbaszek, T. Amand, P. Renucci, V. K. Kalevich, K. V. Kavokin, O. Krebs, P. Voisin, and Y. Masumoto, *Phys. Rev. Lett.* **94**, 116601 (2005).
- ⁷D. Heiss, S. Schaeck, H. Huebl, M. Bichler, G. Abstreiter, J. J. Finley, D. V. Bulaev, and D. Loss, *Phys. Rev. B* **76**, 241306(R) (2007).
- ⁸B. D. Gerardot, D. Brunner, P. A. Dalgarno, P. Öhberg, S. Seidl, M. Kroner, K. Karrai, N. G. Stoltz, P. M. Petroff, and R. J. Warburton, *Nature (London)* **451**, 441 (2008).
- ⁹B. Eble, C. Testelin, P. Desfonds, F. Bernardot, A. Balocchi, T. Amand, A. Miard, A. Lemaître, X. Marie, and M. Chamarro, *Phys. Rev. Lett.* **102**, 146601 (2009).
- ¹⁰J. L. Cheng, M. W. Wu, and C. Lü, *Phys. Rev. B* **69**, 115318 (2004).
- ¹¹M. Trif, P. Simon, and D. Loss, *Phys. Rev. Lett.* **103**, 106601 (2009).
- ¹²H. Wei, M. Gong, G.-C. Guo, and L. He, *Phys. Rev. B* **85**, 045317 (2012).
- ¹³R. J. Warburton, *Nature Mater.* **12**, 483 (2013).
- ¹⁴D. V. Bulaev and D. Loss, *Phys. Rev. Lett.* **95**, 076805 (2005).
- ¹⁵G. Dresselhaus, *Phys. Rev.* **100**, 580 (1955).
- ¹⁶Y. A. Bychkov and E. I. Rashba, *J. Phys. C: Solid State Phys.* **17**, 6039 (1984).
- ¹⁷A. Balocchi, Q. H. Duong, P. Renucci, B. L. Liu, C. Fontaine, T. Amand, D. Lagarde, and X. Marie, *Phys. Rev. Lett.* **107**, 136604 (2011).
- ¹⁸Y. Kanai, R. S. Deacon, S. Takahashi, A. Oiwa, K. Yoshida, K. Shibata, K. Hirakawa, Y. Tokura, and S. Tarucha, *Nature Nanotechnol.* **6**, 511 (2011).
- ¹⁹S. Prabhakar, R. V. N. Melnik, and L. L. Bonilla, *Appl. Phys. Lett.* **100**, 023108 (2012).
- ²⁰S. Prabhakar, R. Melnik, and L. L. Bonilla, *Phys. Rev. B* **87**, 235202 (2013).
- ²¹A. J. Williamson, L.-W. Wang, and A. Zunger, *Phys. Rev. B* **62**, 12963 (2000).
- ²²F. Frasc, B. Eble, P. Desfonds, F. Bernardot, C. Testelin, M. Chamarro, A. Miard, and A. Lemaître, *Phys. Rev. B* **86**, 045306 (2012).
- ²³P. N. Keating, *Phys. Rev.* **145**, 637 (1966).
- ²⁴L.-W. Wang and A. Zunger, *Phys. Rev. B* **59**, 15806 (1999).